

# The Quasi-Continuum of Gamma Rays Following the Decay of Superdeformed Bands in the Hg Region

T. Lauritsen<sup>a</sup>, A. Lopez-Martens<sup>b</sup>, T.L. Khoo<sup>a</sup>, R.V.F. Janssens<sup>a</sup>, M.P. Carpenter<sup>a</sup>, G. Hackman<sup>a</sup>, D. Ackermann<sup>a</sup>, I. Ahmad<sup>a</sup>, H. Amro<sup>a,c</sup>, D.J. Blumenthal<sup>a</sup>, S.M. Fischer<sup>a</sup>, F. Hannachi<sup>b</sup>, A. Korichi<sup>b</sup>, E.F. Moore<sup>c</sup> and D.T. Nisius<sup>a</sup>.

<sup>a</sup> Argonne National Laboratory, Argonne, Illinois 60439, USA. <sup>b</sup> Centre de Spectrométrie Nucléaire et de Spectrométrie de masse, IN2P3-CNRS, bat 104-108, F-91405 Orsay, France and Institut de Physique Nucléaire, F-91406, Orsay Cedex, France. <sup>c</sup> North Carolina state University, Raleigh, North Carolina 27695, USA

The quasi-continuum part of the spectrum associated with the decay-out of the yrast superdeformed band in <sup>194</sup>Hg has been extracted. It has for the first time been possible to compare the spin and excitation energy determined from the analysis of the quasi-continuum  $\gamma$  rays to the exact result obtained from the one-step linking transitions.

## INTRODUCTION

About 175 superdeformed (SD) bands have by now been found in the A=80,150 and 190 mass regions; yet only a few of these have been firmly linked to the normal deformed (ND) states they decay into. Thus, fundamental quantities such as *spin*, *parity* and *excitation energy* have not been experimentally determined for the vast majority of the SD bands. In order to address issues of great recent interest such as: [i] the presence of identical SD bands, [ii] the magnitude of shell corrections at large deformation, [iii] the mechanisms responsible for the sudden decay-out of the SD bands, [iv] the description of pairing and level densities in the SD well, some or all of those quantities must be determined for as many SD bands as possible.

Recently, one-step decays out of the yrast SD bands in <sup>194</sup>Hg and <sup>194</sup>Pb have been reported [1,2]. One-step decays allow for an unambiguous determination of the spin, parity and excitation energy of the states in a SD band. However, the intensity of these special decay branches is only a fraction of that of the SD band itself, and most of the decay proceeds through a quasi-continuum (QC) of  $\gamma$  rays. Moreover, the strength of one-step decays varies considerably from nucleus to nucleus and may be subject to Porter-Thomas fluctuations. Therefore, it may not always be possible to observe one or two-step decays – even when data of very good statistics are available. In such cases, the analysis of the QC provides an alternative way to determine the spin and energy of the SD bands, provided that the analysis methods are proven to be reliable.

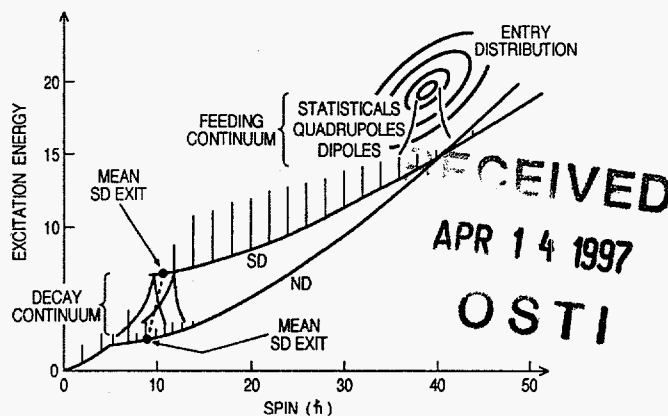


FIG. 1. Schematic diagram of the feeding and decay of SD bands. Gamma emission starts from the entry distribution. After emission of statistical, quadrupole and M1/E2 dipole QC  $\gamma$  rays, the deexcitation cascades are trapped either in the ND or SD wells, where discrete gamma rays are emitted. If a  $\gamma$  cascade is trapped in the SD well, QC  $\gamma$  rays are also emitted when the SD band decays into the ND states.

A schematic diagram of the feeding and decay of a SD band in figure 1 shows that there are two components to the QC: [i] one associated with the feeding of the SD states and [ii] the other originating from the decay towards the yrast states [3]. A simple way to assess where the decay QC  $\gamma$  rays are located is to compare coincidence spectra gated on ND and SD transitions. Only the spectra gated on SD  $\gamma$  rays should have the 'extra' QC component from the decay-out to ND states at or near the yrast line. Such a comparison for <sup>194</sup>Hg is given in figure 2 (with the discrete peaks left in the spectrum). It is clearly seen in the figure that extra strength is present in the SD gated spectrum above 1 MeV - exactly where the  $\gamma$  rays from a statistical decay of the levels at the bottom of the SD band are expected [4]. The spectrum has close similarities with that reported earlier for <sup>192</sup>Hg [3]. In particular, as in the latter nucleus, the excess strength above 1 MeV is ascribed to the decay out of the SD band.

Differences below 1 MeV are also seen in figure 2, but those have to do with the different paths the nucleus takes in the feeding of the ND and SD bands.

MASTER DISTRIBUTION OF THIS DOCUMENT IS UNLIMITED

The submitted manuscript has been authored by a contractor of the U. S. Government under contract No. W-31-109-ENG-38. Accordingly, the U. S. Government retains a nonexclusive, royalty-free license to publish or reproduce the published form of this contribution, or allow others to do so, for U. S. Government purposes.

## **DISCLAIMER**

**This report was prepared as an account of work sponsored by an agency of the United States Government. Neither the United States Government nor any agency thereof, nor any of their employees, make any warranty, express or implied, or assumes any legal liability or responsibility for the accuracy, completeness, or usefulness of any information, apparatus, product, or process disclosed, or represents that its use would not infringe privately owned rights. Reference herein to any specific commercial product, process, or service by trade name, trademark, manufacturer, or otherwise does not necessarily constitute or imply its endorsement, recommendation, or favoring by the United States Government or any agency thereof. The views and opinions of authors expressed herein do not necessarily state or reflect those of the United States Government or any agency thereof.**

**DISCLAIMER**

**Portions of this document may be illegible in electronic image products. Images are produced from the best available original document.**

In the feeding of the yrast SD band, about six  $\gamma$  rays of stretched E2 character are emitted while the nucleus decays through excited, damped SD bands [5]. A pronounced 'E2-bump' is therefore seen in the SD gated spectrum (and it should result in ridges in coincidence matrices). On the other hand, the cascades feeding the ND bands involve less collective states and, as a result, the E2-bump associated with this decay mode is much smaller.

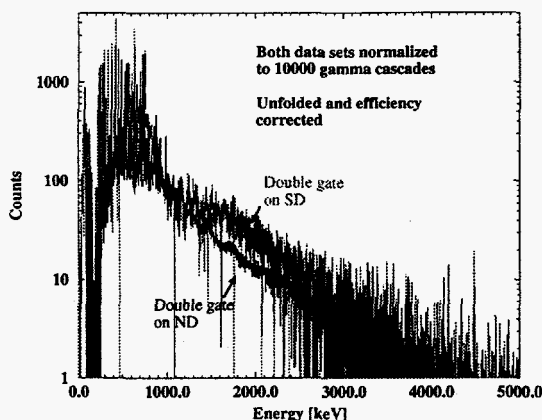


FIG. 2. Comparison of ND and SD gated coincidence spectra in  $^{194}\text{Hg}$ . The spectrum gated on the the SD band shows additional strength above 1 MeV from the QC  $\gamma$  rays associated with the decay of the SD band to ND states.

By extracting the QC  $\gamma$  rays in coincidence with the SD band, it is possible to deduce both the spin and energy of the SD band at the point of decay. When the QC intensity is normalized to the number of  $\gamma$  cascades, the area of the spectrum determines the average multiplicity, i.e., the number of  $\gamma$  rays involved in the decay. Similarly, the mean energy of the decay-out QC determines the average energy removed by these  $\gamma$  rays. Thus, by simple multiplication of these two quantities, the mean energy removed by the QC is established. It is likewise possible to determine the average amount of spin removed by the  $\gamma$  rays.

From the intensities, spins and energies of the ND transitions in coincidence with the SD band, the average spin and energy corresponding to the entry into the ND states can be derived (see figure 1). By vectorially adding the spin and energy removed by the QC to the mean ND entry-point, the *mean SD exit-point* can be found. From this information the spins and energies of the SD band levels can be deduced, once the branching ratios between in-band and out-of-band decay are taken into account for the lower SD states.

## THE EXPERIMENT

The SD band in  $^{194}\text{Hg}$  was populated using the reaction  $^{150}\text{Nd}(^{48}\text{Ca},4n)$ . The beam, delivered by the 88" cyclotron at LBNL, had an energy of 202 MeV. A total of  $1.9 \times 10^9$  quadruple or higher fold coincidence events was collected with GAMMASPHERE, which at the time comprised 85 detectors. The target consisted of a  $1.2 \text{ mg/cm}^2$   $^{150}\text{Nd}$  layer evaporated on a thick Au backing, which ensured that all  $\gamma$  rays associated with the decay-out of the SD band would not be subject to any Doppler shift.

## THE EXTRACTION OF THE QC

In order to extract the QC  $\gamma$  rays from the total spectrum, the data must be processed carefully in a number of steps. Double coincidence gates were placed on SD transitions in order to obtain SD spectra almost free of contaminant coincidences, yet with sufficient statistics for an angle sort. Only 9 of 36 possible double gate combinations were deemed clean enough for use in this analysis. (Triple gating would have provided even cleaner spectra; but the statistics in the angle sort would have been marginal.) Correct background subtraction of the double-gated spectra is vital. The FUL method [6] developed at ANL was used to subtract background-background and peak-background contributions. The data was also sorted according to the prescription in [7] in order to avoid 'spikes' in the gated spectra. In addition, any lines left in the spectra as a result of contaminant coincidences (despite careful selection of gates) were identified, characterized and subtracted.

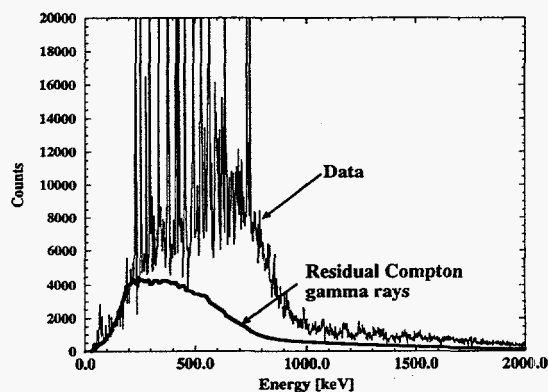


FIG. 3. Residual Compton events in a typical spectrum. The figure shows a gated spectrum before unfolding and the lower solid curve shows the residual Compton events subtracted by the procedure described in [7], using a measured response function for GAMMASPHERE.

The angle sorted spectra were corrected for the response of the GAMMASPHERE array in successive steps described below. First the contributions due to true coincidence summing was removed following a prescription by Radford [8]. The  $\gamma$  rays generated from neutron interactions in the Ge detectors (mostly in the forward direction) were subtracted next. This contribution is small (2-3%) and has very little impact in the energy region of the decay-out  $\gamma$  rays. A more significant correction is the removal of the Compton events in the spectra. Even with efficient BGO shields, about 1/2 of all Compton events is not suppressed and to extract the true QC, it is necessary to subtract these unwanted  $\gamma$  rays.

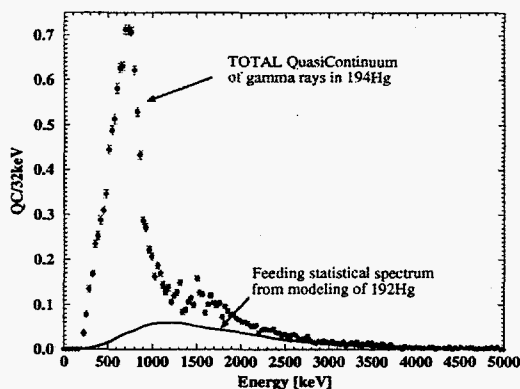


FIG. 4. The total QC after discrete peaks have been removed and the spectra contracted to 32 keV/ch. Also shown is the calculated statistical spectrum from  $^{192}\text{Hg}$ .

By measuring the spectra from single-line and two-line coincidence sources placed at the target position, the response function of GAMMASPHERE was carefully measured. Using the unfolding procedure described in [8], which interpolates between the response-measurement at discrete energies, the residual Compton  $\gamma$  rays for the entire spectrum were deduced and subtracted. Figure 3 shows a typical spectrum before the unfolding, together with the residual events left in the spectrum despite Compton suppression (lower curve). It is clearly seen that the procedure by Radford works well, even in the low energy region where it is most difficult to unfold.

Next, the spectra were corrected for detector efficiency, the discrete  $\gamma$  rays were removed and the spectra were contracted to 32keV/ch. The remaining QC  $\gamma$  rays consist of the three feeding QC components, i.e., [i]statistical, [ii]quadrupole and [iii]dipole transitions from the last step in the feeding [3]. The fourth QC component is the sought-after decay-out spectrum which will be extracted by subtracting the feeding statistical and quadrupole components.

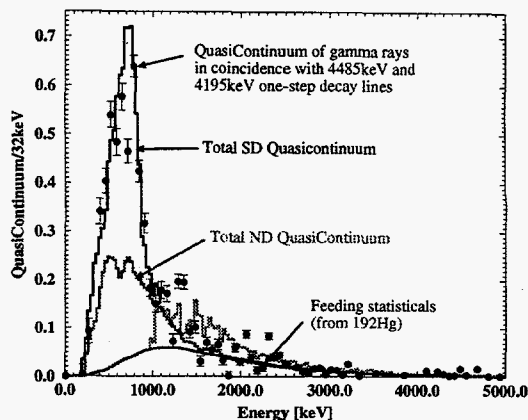


FIG. 5. The QC  $\gamma$  rays obtained from double gates placed on the one-step decay-out lines and SD lines in  $^{194}\text{Hg}$  (data with error bars). Also shown are the total SD and ND QC spectra and the calculated statistical spectrum from  $^{192}\text{Hg}$ .

Finally, the QC spectra are normalized so that the area of the  $2^+ \rightarrow 0^+$  ground-state transition in the spectrum is unity, after corrections for internal conversion, angular distribution and changes to the intensity due to isomers have been taken into account. After this normalization, it follows that any area is equal to multiplicity, since the spectrum represents an average  $\gamma$  cascade. Figure 4 shows the total QC spectrum corrected for angular distribution effects ('A0' spectrum).

#### THE STATISTICAL FEEDING COMPONENT

In reference [5], the statistical spectrum feeding the SD band in  $^{192}\text{Hg}$  was calculated using as input the experimentally measured entry states distribution. This statistical spectrum is also expected to be applicable in the case of  $^{194}\text{Hg}$ . Because the one-step decay lines have been observed in this nucleus [1], it is possible to confirm experimentally this hypothesis by extracting the QC in coincidence with the one-step decay-out lines. This spectrum should *not* contain the decay QC and thus, at higher energies, it should follow the calculated statistical spectrum rather than the total QC.

The sum of coincidence spectra, with double coincidence gates placed on the one-step decay-out  $\gamma$  rays and the SD lines, has been corrected for the response of GAMMASPHERE. It is presented in figure 5 overlaid with the total QC spectrum and the calculated statistical spectrum. Despite low statistics, the agreement between this spectrum and that obtained with double gates on SD lines is very good over the 'E2-bump' region, although there appears

to be some contaminant lines just above 1 MeV. At higher energies, the data are seen to follow the statistical spectrum, thus justifying our hypothesis. It should be noticed that the QC spectrum gated on ND transitions also follows the calculated statistical spectrum at higher energies, again suggesting that the calculated statistical spectrum from  $^{192}\text{Hg}$  can be used in  $^{194}\text{Hg}$ . The calculated statistical spectrum is subtracted from the total QC spectrum shown in figure 4, thus eliminating one of the four QC components.

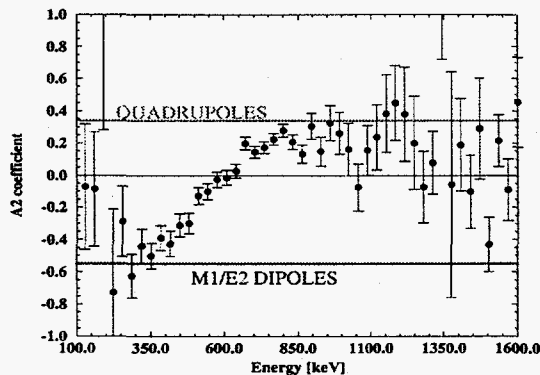


FIG. 6. Angular distribution coefficients, channel by channel, for the QC after the statistical  $\gamma$  rays have been subtracted.

### THE QUADRUPOLE FEEDING COMPONENT

After the statistical spectrum has been subtracted, the A2 angular distribution coefficient of the remainder of the spectrum can be found channel by channel: the result is shown in figure 6. If the coefficient is close to the calculated E2 limit of  $\approx +0.34$ , the QC content of the channel is assumed to be of pure E2 character. Conversely, if the coefficient is close to the large negative value of the M1/E2 dipole transitions,  $\approx -0.55$ , the channel content is taken to be of pure M1/E2 dipole character. (In the analysis, it is assumed that there is no remaining E1 strength in the spectrum up to  $\approx 1\text{MeV}$  following the subtraction of the statistical spectrum). For A2 coefficients with values between those extremes, the counts in the channels are split proportionally between the two contributions. In this way, the E2 QC-component was extracted. The QC quadrupole  $\gamma$  rays are emitted early in the  $\gamma$  cascade, while the nucleus is still in flight, with a velocity close to the maximum recoil velocity. Hence, the A2 angular distribution analysis is performed on spectra transformed into the center of mass system, and the E2 QC component is subtracted from the spectra of

each detector ring after corrections for Doppler shift, angular distribution and relativistic aberration.

### SPIN AND ENERGY OF THE SD BAND

After both the statistical and quadrupole components from the feeding have been subtracted, the remaining spectrum still consists of the M1/E2 feeding  $\gamma$  rays and the sought after QC decay-out  $\gamma$  rays. There are clear indications of two components in fig. 7. The low energy component has large negative A2 coefficients (indicating M1/E2 nature) and the upper component resembles the 'extra' strength shown earlier in the SD-ND gate comparison in figures 2. Thus, the upper component ( $\approx 1\text{MeV}$  and higher) is assigned to the decay out process as it was in reference [3] for the case of  $^{192}\text{Hg}$ .

The mean energy of this decay-out component is 1.8(1) MeV and its area, equal to multiplicity, is 2.3(2). Therefore, it immediately follows that this QC of  $\gamma$  rays removes 4.1(4) MeV of energy. From Monte Carlo simulations [5] of a statistical decay at the proper spin and energy it is found that, on the average,  $0.5(2)\hbar$  of spin is removed by these  $\gamma$  rays. Thus,  $1.1(4)\hbar$  of spin is removed by the decay  $\gamma$  rays in this QC component.

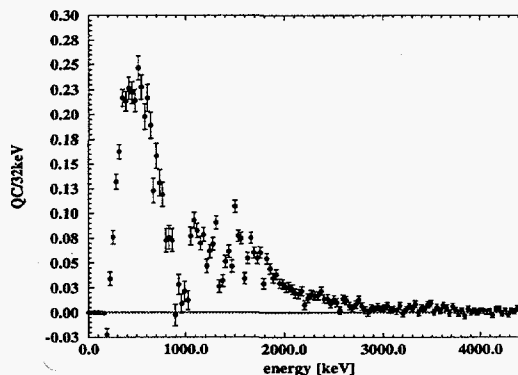


FIG. 7. The QC  $\gamma$  rays in  $^{194}\text{Hg}$  after both the feeding statistics and quadrupoles have been subtracted. The spectrum shows the dipole component of the feeding at low energies and the decay-out QC component at higher energies.

Some SD decay paths will feed into states located above the yrast line, which are either not populated or populated weakly when ND bands are feed. The  $\gamma$  rays from the decay of these states can be found by close inspection of all the discrete  $\gamma$  rays that were removed in the early stages of the analysis; but have not been assigned in the ND level scheme. (By placing coincidence gates on those candidate transi-

tions, it was checked that the lines are not the result of contaminant coincidences). In [3] it was estimated that, on the average, half (multiplicity 0.5(2)) of the  $\gamma$  cascades deexciting the SD band goes through such states and gives rise to discrete lines in a region up to 1 MeV. These  $\gamma$  rays need to be taken into account when the spin and energy of the SD band are calculated. In total, these  $\gamma$  rays remove 0.8(3) $\hbar$  and 0.3(1) MeV which must be vectorially added to the 'regular' QC spin and energy vector in order to find the mean SD exit-point (see figure 1).

From the intensities, spin and energies of the known ND lines in coincidence with the SD band, it is found that the entry point of the SD band into the known ND states is located at a spin of 9.3(5) $\hbar$  and an energy of 2.4(1) MeV. The errors quoted here are due [i] to difficulties in assigning intensities to some low energy lines which are not observed well with GAMMASPHERE, and [ii] to the presence of two low spin isomers in the yrast level structure, which complicate the determination of  $\gamma$ -ray intensities for transitions involved in their deexcitation.

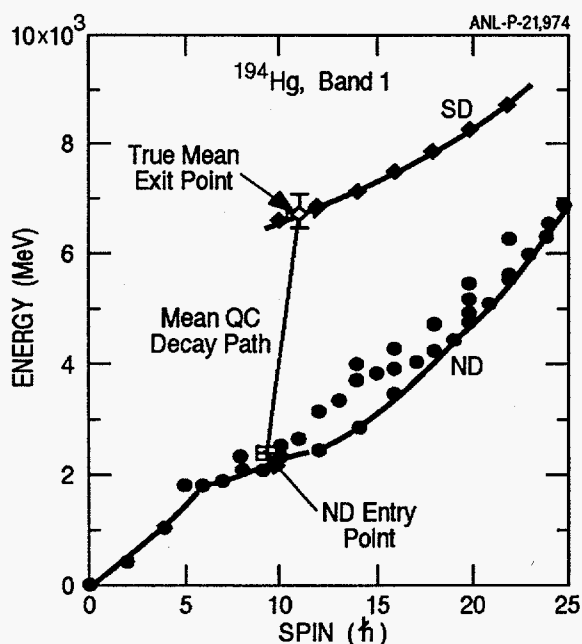


FIG. 8. The mean SD exit-point found by adding the spin and energy removed by known ND lines, new unassigned ND lines and the decay-out QC  $\gamma$  rays.

By adding all the contributions; i.e., the known ND lines, the new weak ND lines just discussed and the decay-out QC  $\gamma$  rays, the *mean SD exit-point* is determined. The result is displayed in figure 8. In the figure, a vector characterizing the mean QC decay path obtained as described above links the entry point into the ND levels and the SD exit point. It is this SD exit-point located at 11.1(7) $\hbar$  and 6.8(3)

MeV that can be compared directly to the result from the one-step decays [1]. According to the analysis in [1], 48% of the decay of the SD band occurs from the 6.88 MeV  $12^+$  state and 52% from the 6.63 MeV  $10^+$  state, establishing the true mean SD exit-point as: (11.0 $\hbar$ , 6.8 MeV).

The main conclusion of the present analysis is as follows: *the mean exit-point measured from the QC is in remarkably good agreement with the exact result established from the one-step decay  $\gamma$  rays.* Another way to present this result is to calculate the spin and energy the QC method would assign to the ' $10^+$ ' state: i.e.,

$$I = 10.1(7)\hbar \quad [\text{true: } 10\hbar]$$

$$E = 6.7(3) \text{ MeV} [\text{true: } 6.6 \text{ MeV}]$$

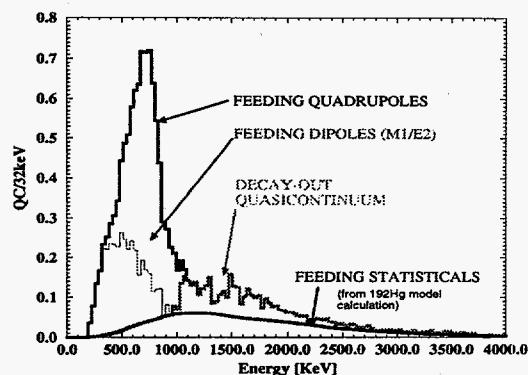


FIG. 9. All the QC components in the feeding and decay of the yrast SD band in  $^{194}\text{Hg}$ .

## THE DECAY MECHANISM

As the nucleus removes spin and energy by emitting stretched E2  $\gamma$  rays along the SD yrast line, the SD states become hotter and hotter with respect to the ND yrast line (see figure 1). Thus, the ratio of ND to SD level densities increases as the nucleus decays in the SD well. Moreover, the in-band transition rates diminish because of the rapidly decreasing transition energies. In addition, there is also evidence that the barrier height is reduced at lower spin. A SD band decays to the ND states when the states in the SD band acquire a sufficient component of the wave-function of the hot ND states located on the other side of the barrier separating the two wells [3,5,9]. Because of the exponential dependence of the mixing as a function of spin, the decay happens suddenly, over a few SD states.

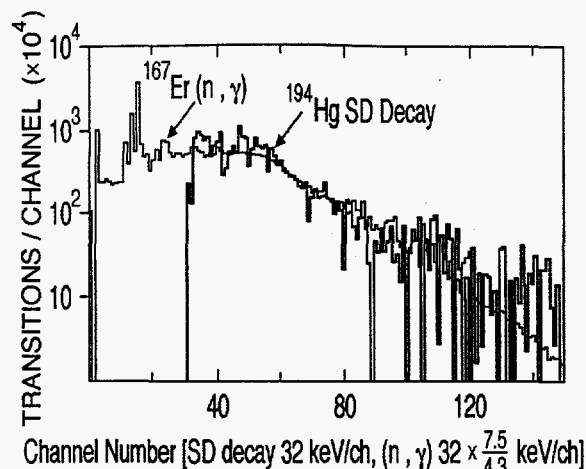


FIG. 10. The QC  $\gamma$  rays from the decay of the yrast SD band in  $^{194}\text{Hg}$  overlaid with the gain adjusted QC  $\gamma$  rays following neutron capture in  $^{167}\text{Er}$ .

It follows from the above picture of the decay of a SD band that the spectrum of the  $\gamma$  rays emitted in the decay process is governed by the levels in the ND well. The end-point of the QC spectrum is determined by the excitation energy of the SD states. Thus, a decay from a fission isomer or from a state populated in neutron capture is expected to be characterized by a decay spectrum of the same form as the one seen in this work. This follows since all these processes are governed by statistical emission of  $\gamma$  rays from 'sharp' states, i.e. states with a well defined energy.

The QC  $\gamma$  rays following neutron capture in  $^{167}\text{Er}$  have been measured using Tessa-3 at Brookhaven [10]. The spectrum after unfolding, efficiency correction and removal of the discrete peaks below 600 keV is presented in figure 10, where it is overlaid with the SD decay-out QC discussed in this paper. Since the sharp states populated by neutron capture are located at higher energy than the SD levels (7.7 MeV vs. 4.3 MeV), the neutron capture spectrum was gain-adjusted so that its end-point matched that of the SD decay spectrum. The similarity (in shape and magnitude) of the two spectra is striking and suggests that, in both cases the decay is governed by the same mechanism, statistical decay from hot 'compound' states.

## CONCLUSIONS

It has been shown that the *spin* and *excitation energy* of the yrast SD band in  $^{194}\text{Hg}$  which are extracted from the analysis of the QC  $\gamma$  rays from the decay-out process are in excellent agreement with the exact result obtained from one-step decay transitions. Thus, spins and excitation energies can be

determined with this method in cases where Porter-Thomas fluctuations or other conditions prevent the observation of direct one-step or two-step decays from SD bands.

| component     | $\bar{m}$ | $\bar{e}$   |
|---------------|-----------|-------------|
| Statisticals  | 3.2       | 1.68 MeV    |
| Quadrupoles   | 6.0(1)    | 0.73(1) MeV |
| M1/E2 dipoles | 3.37(6)   | 0.54(1) MeV |
| Decay-out QC  | 2.28(6)   | 1.77(6) MeV |
| new ND lines  | 0.5(2)    | 0.6(2) MeV  |

TABLE I. The mean multiplicities and mean energies of the QC components in  $^{194}\text{Hg}$ . Only statistical errors are given. Also listed are the current results of the cataloging of the new ND states (where the error bars are dominated by systematics).

Figure 9 shows all the components of the QC: [i]the statistical, [ii]quadrupole and [iii]dipole  $\gamma$  rays associated with the feeding and [iv]the QC  $\gamma$  rays from the decay-out of the SD band. Table I shows the mean multiplicities and mean energies of all these components.

Work is still in progress to improve on the errors associated with various contributions by [i]gathering more statistics, [ii]removing contaminant coincidences in the spectra and [iii] doing a more thorough cataloging of the new, unplaced ND lines. The latter process has already yielded more two-step decays which have been added to the decay level scheme in reference [1].

This work was supported in part by the U.S. Dept. of Energy, under Contract No. W-31-109-ENG-38.

- [1] T.L. Khoo *et al.*, Phys. Rev. Lett. **76**(1996)1583 and G. Hackman, this conference
- [2] A. Lopez-Martens *et al.*, Phys. Lett. **B380**(1996)18, Hannachi *et al.*, this conference
- [3] R.G. Henry *et al.*, Phys. Rev. Lett. **73**(1994)777
- [4] T. Døssing *et al.*, Phys. Rev. Lett. **75**(1995)1276
- [5] T. Lauritsen *et al.*, Phys. Rev. Lett. **69**(1992)2479
- [6] B. Crowell *et al.*, Nucl. Instr. & Methods **A235**(1995)575
- [7] C.W. Beausang *et al.*, Nucl. Instr. & Methods **A364**(1995)560
- [8] D.C. Radford *et al.*, Nucl. Instr. & Methods **A258**(1987)111
- [9] E. Vigezzi *et al.*, Nucl. Phys. **A520**(1990)179c and E. Vigezzi *et al.*, Phys. Lett. **B249**(1990)163
- [10] F. Soramel *et al.* to be published